IEEE Access
Multidisciplinary | Rapid Review | Open Access Journal

Received September 1, 2019, accepted September 19, 2019, date of publication October 4, 2019, date of current version October 22, 2019.

Digital Object Identifier 10.1109/ACCESS.2019.2945530

Analytic Calculation of Geoelectric Fields due to Geomagnetic Disturbances: A Test Case

DAVID H. BOTELER[1], (Senior Member, IEEE), RISTO J. PIRJOLA[1], AND LUIS MARTI[2], (Fellow, IEEE)

[1]Natural Resources Canada, Ottawa, ON K1A 0E7, Canada
[2]L Marti Consulting, Toronto, ON L5L 2Z7, Canada

Corresponding author: David H. Boteler (david.boteler@canada.ca)

This work was performed as part of Natural Resources Canada's Public Safety Geoscience Program. Contribution number: 20180403.

ABSTRACT Geomagnetic field variations produce geoelectric fields that can affect the operation of technological networks at the Earth's surface, including power systems, pipelines, phone cables and railway circuits. To assess the geomagnetic hazard to this technology, it is necessary to model the geomagnetically induced currents (GIC) produced in these systems during geomagnetic disturbances. This requires use of geomagnetic data with appropriate Earth conductivity models to calculate the geoelectric fields that drive GIC. To provide a way of testing geoelectric field calculation software, we provide a benchmark test case by defining a synthetic geomagnetic field variation and deriving exact analytic expressions for the Earth response based on both uniform and layered Earth conductivity models. These are then used to provide exact analytic expressions for the geoelectric fields that would be produced by the synthetic geomagnetic field variation. The synthetic geomagnetic data can be used as input to numerical geoelectric field calculation software, the output of which can be tested by comparison with the analytically-generated geoelectric fields.

INDEX TERMS Geoelectric fields, geomagnetic disturbances, power systems.

I. INTRODUCTION

Geomagnetic field variations induce geoelectric fields in the Earth and in man-made conductors at the Earth's surface such as power systems, pipelines, phone cables and railway circuits, e.g. [1]. The geoelectric fields produce currents and voltages in these technologies that can damage equipment and create problems for system operation. There is a long history of geomagnetic effects on these ground-based systems [2]. Cable systems have been put out of operation [3]; and changes in pipeline potentials observed in many parts of the world are a concern because of their possible contribution to corrosion and disturbance to corrosion control [4]. However, the greatest effects have been observed on power transmission systems. Here, the geomagnetically induced currents (GIC) driven by the geoelectric field flow through power transformers where they cause asymmetrical saturation of the transformer core resulting in transformer heating, generation of harmonics and increased reactive power consumption by the transformers. These can lead to transformer damage [5]–[7], mis-operation of protective relays [8], and, in a worst case, power blackouts [9].

To understand the geomagnetic effects on ground-based systems, considerable work has gone into modelling the response of the systems to geomagnetic field variations. That work can be split into two parts, e.g. [1], [10]: the ''geophysical'' part involving use of geomagnetic field recordings and an Earth conductivity model to calculate the geoelectric fields produced at the surface of the Earth; and the ''engineering'' part which uses the calculated geoelectric fields as input to the appropriate network model to calculate the currents and voltages in the system. Such calculations provide important information that can be used in system design or planning ameliorating actions [11], [12]. With engineering decisions and associated expenditure being based on this modelling, it is, of course, important that the calculations give the correct results. The fundamental theory is well established and tested, however, there is still a need to ensure that software implementations of the modelling theory perform as intended. A benchmark model has been developed to provide a test case for modelling GIC in power systems [13], and a model and results have been provided for the calculation of potential variations on pipelines [14]. However, there has never been a

The associate editor coordinating the review of this manuscript and approving it for publication was Ramazan Bayindir.

test case for the geophysical part of the problem: the calculation of the geoelectric fields produced by geomagnetic field variations.

The purpose of this paper is to present an exact analytic solution and provide a test case for the calculation of geoelectric fields. First we explain the process of geomagnetic induction in the Earth and derive the equations relating the geoelectric and geomagnetic fields at the Earth's surface. These are then used to calculate the Earth transfer functions for two models: a) an Earth with uniform conductivity, and b) an Earth represented by multiple layers with different conductivities to represent the change in Earth conductivity with depth. Then we create a dataset of a synthetic geomagnetic field variation and use this with the two Earth model transfer functions to produce an exact analytic solution for the geoelectric field in each case. The synthetic geomagnetic field variation and the analytic solutions for the geoelectric field provide benchmark results against which numerical calculations can be tested.

II. GEOMAGNETIC INDUCTION

A. BASIC PROCESSES

Geomagnetic field variations originate from electric currents in the ionosphere and magnetosphere above the Earth. The incident geomagnetic field variations induce electric currents in the Earth that, themselves, create a magnetic field. Thus the geomagnetic field variations observed at the Earth's surface are comprised of an ''external'' part from the ionospheric and magnetospheric sources and an ''internal'' part produced by the induced currents. Within the Earth the magnetic field created by the induced currents acts to cancel the external magnetic field variations, leading to a fall-off of the magnetic field amplitude with depth within the Earth – an example of the ''skin depth'' effect. The geoelectric field associated with the induced currents depends on the Earth conductivity and frequencies of the geomagnetic field variations. At the frequencies of concern to ground infrastructure, 10^{-5} to 1 Hz (i.e. periods of 1 sec to 24 hrs), the fields penetrate tens to hundreds of kilometres into the Earth, so the Earth conductivity down to these depths has to be taken into account in the calculation of the geoelectric field.

B. ELECTROMAGNETIC THEORY

The theory for geomagnetic induction in the Earth relating the electric and magnetic fields at the Earth's surface started with the work of Cagniard [15] and Wait [16], was developed by Price [17] and Wait [18] and has evolved into the well-established Magnetotelluric (MT) geophysical technique [19], [20]. The theory now includes methods that take account of the effects of the ionospheric-magnetospheric source structure e.g. [21], [22] and of the three-dimensional (3-D) conductivity structure of the Earth, see review in [23] and references therein. However, for many practical applications, where detailed information on the magnetic source fields or the Earth conductivity structure may not be available, geoelectric field calculations can be made by assuming a spatially uniform ''*plane wave*'' magnetic source field and a one-dimensional (1-D) model of the Earth conductivity structure that takes account of the variation of conductivity with depth but neglects lateral variations in conductivity. The methods for making these calculations have been presented by many authors e.g. [24]–[26]. We summarize the derivation here, in order to provide a complete derivation, starting from first principles, of the analytic solution for the geoelectric field test case.

The relations between the geoelectric (**E**) and geomagnetic (**B**) fields in the Earth are governed by Maxwell's equations. For the frequencies of concern, mentioned in Section II.A, and the conductivities, σ, in the Earth, the displacement currents are negligible. Then, assuming a time (t) variation of the form $e^{i2\pi ft}$ (f = frequency), Maxwell's equations can be written as

$$\nabla \times \mathbf{E} = -i2\pi f \mathbf{B} \tag{1}$$

$$\nabla \times \mathbf{B} = \mu_0 \sigma \mathbf{E} \tag{2}$$

where the magnetic permeability is set equal to the free space value $\mu_0 = 4\pi \cdot 10^{-7}$ H/m. In a region of uniform conductivity σ, equation (2) implies that $\nabla \cdot \mathbf{E} = 0$. Then taking the curl of (1) and using (2) gives the diffusion equation

$$\nabla^2 \mathbf{E} = k^2 \mathbf{E} \tag{3}$$

where the propagation constant k is defined by

$$k = \sqrt{i2\pi f \mu_0 \sigma} \tag{4}$$

Let us use the standard geoelectromagnetic coordinate system, in which the Earth's surface is the xy plane and the x, y and z axes point northwards, eastwards and downwards, respectively. We assume that the horizontal variations of the geoelectric and geomagnetic (variation) fields are much less than the variation with depth (''*plane wave assumption*''), i.e. the fields practically only depend on the z coordinate. Then equation (3) reduces to

$$\frac{d^2 \mathbf{E}}{dz^2} = k^2 \mathbf{E} \tag{5}$$

Equation (5) enables solving **E** in the Earth, and equation (1) can then be used for determining **B**.

The relation between the orthogonal horizontal geoelectric field, $E = E(f)$, and magnetic field, $B = B(f)$, components in the frequency domain at the Earth's surface is, by definition, the ''*Transfer Function*'' $K = K(f)$, i.e.

$$E(f) = K(f)\, B(f) \tag{6}$$

Here $E(f)$ and $B(f)$ form a right-handed pair where the electric field is rotated 90 degrees counterclockwise from the direction of the magnetic field. Thus, $K(f)$ gives the relation between either $E_x(f)$ and $B_y(f)$ or $-E_y(f)$ and $B_x(f)$.

It is worth pointing out that the transfer function $K(f)$ is closely related to the ''*Surface Impedance*'' $Z(f)$ commonly used in magnetotelluric studies: $Z(f) = \mu_0 K(f)$. The electric

field can also be related to the rate of change of the magnetic field, $g(t) = \mathrm{d}B(t)/\mathrm{d}t$. Noting that in the frequency domain $g(f) = \mathrm{i}2\pi f B(f)$, we obtain from (6)

$$E(f) = K(f)\,B(f) = \frac{K(f)}{i2\pi f} i2\pi f B(f) = C(f)\,g(f) \quad (7)$$

where $C(f)$ given by

$$C(f) = \frac{K(f)}{i2\pi f} \quad (8)$$

is called the "*Magnetotelluric Relation*".

If the conductivity, σ, is spatially constant within a region, then the propagation constant k is independent of z, and solving $E = E(f)$ from equation (5) gives

$$E = Se^{-kz} + Re^{kz} \quad (9)$$

where S and R are related to the amplitudes of downward and upward propagating waves, respectively. Substituting E from (9) into (1) yields

$$B = \frac{k}{i2\pi f}\left(Se^{-kz} - Re^{kz}\right) \quad (10)$$

C. UNIFORM EARTH

Let us first assume that the Earth is uniform, i.e. σ is spatially constant in the half-space $z > 0$. Equations (9) and (10) give the solutions for the electric and magnetic fields in the Earth. However, in this case, there is no bottom plane for reflection, which means that there is no upward propagating wave, and so $R = 0$. Consequently (9) and (10) become

$$E = Se^{-kz} \quad (11)$$

$$B = \frac{k}{i2\pi f} Se^{-kz} \quad (12)$$

Utilizing the definition (6) of the transfer function $K(f)$, equations (11) and (12) give

$$K(f) = \frac{E(z=0)}{B(z=0)} = \frac{i2\pi f}{k} = \sqrt{\frac{i2\pi f}{\mu_0 \sigma}} \quad (13)$$

D. LAYERED EARTH

In practice the Earth conductivity varies in all directions, but the greatest variation is with depth and the Earth is often represented by a 1-D model comprised of N horizontal layers with specified conductivities (σ_1,…, σ_N) and thicknesses (l_1,…, l_N). The bottom layer N is a uniform half-space, so $l_N = \infty$. As above, we assume that the horizontal variations of the geoelectric and geomagnetic fields are much less than the variation with depth, i.e. the fields are considered to only depend on the z coordinate. Then the electric and magnetic fields are expressed by (9) and (10) in each layer with $k = k_n = \sqrt{i2\pi f \mu_0 \sigma_n}$ ($n = 1,\ldots, N$). Thus

$$E = S_n e^{-k_n z} + R_n e^{k_n z} \quad (14)$$

$$B = \frac{k_n}{i2\pi f}\left(S_n e^{-k_n z} - R_n e^{k_n z}\right) \quad (15)$$

where $0 \le z \le l_n$ and S_n and R_n are the amplitudes of a downward and upward propagating wave at the top surface of layer n. (Note that here, for each layer, the location of $z = 0$ is set at the top surface of each layer, not at the Earth's surface.) As the bottom layer N is a half-space, $R_N = 0$.

We now outline derivation of transfer function $K = K(f)$ for the N-layer Earth. We can assume that $N > 1$ since if $N = 1$ the Earth is uniform, which was already discussed in Section II.C. Let us denote the ratio of E to B at the top surface of layer n by K_n. As layer $n = N$ is a uniform half-space, the value of K_N is directly obtained from formula (13), which expresses the uniform-Earth transfer function. Thus

$$K_N = \frac{i2\pi f}{k_N} = \sqrt{\frac{i2\pi f}{\mu_0 \sigma_N}} \quad (16)$$

In each layer the solutions of (14) and (15) for the top of the layer ($z = 0$) and bottom of the layer ($z = l_n$) give

$$K_n = \eta_n \frac{S_n + R_n}{S_n - R_n} \quad (17)$$

$$K_{n+1} = \eta_n \frac{S_n e^{-k_n l_n} + R_n e^{k_n l_n}}{S_n e^{-k_n l_n} - R_n e^{k_n l_n}} \quad (18)$$

where $\eta_n = \frac{i2\pi f}{k_n}$ is the "*Characteristic Function*" of layer n.

Solving R_n from (18) and substituting into (17), as shown in [27], gives

$$K_n = \eta_n \frac{K_{n+1}\left(1 + e^{-2k_n l_n}\right) + \eta_n\left(1 - e^{-2k_n l_n}\right)}{K_{n+1}\left(1 - e^{-2k_n l_n}\right) + \eta_n\left(1 + e^{-2k_n l_n}\right)} \quad (19)$$

Formula (19) is a recursive relation for calculating K_n at the top surface of layer n from K_{n+1} at the top surface of the underlying layer $n+1$. The initial value in the application of formula (19) is K_N given by equation (16). This is the input to calculate K_n at the top surface of the next layer up. This is then used in the calculation for the next layer, and so on, up to the Earth's surface. The final value is the transfer function $K = K_1$ relating $E = E(f)$ and $B = B(f)$ at the Earth's surface.

Formulas (13) and (19) give the transfer function as complex values at each frequency. The amplitude and phase are easily calculated from the real and imaginary components [27]. It should be noted that the multi-layer transfer function is exact, as is the uniform-Earth transfer function, but in the multi-layer case the transfer function can only be expressed by the recursive relation (19) with the initial value from (16) whereas the transfer function for a uniform Earth has a simple explicit formula (13).

By taking the Fourier transform, any time variation of the geomagnetic field can be decomposed into its frequency components; each multiplied by the corresponding transfer function values from the above formulas to give the geoelectric field frequency components. The inverse Fourier transform, i.e. summation of these components, then gives the electric field in the time domain [26].

III. SYNTHETIC TEST MAGNETIC FIELD VARIATION

To test the calculation of geoelectric fields using the above relations, we need a specified geomagnetic field variation

TABLE 1. Parameters of synthetic magnetic field variation.

m	A_m (nT)	Φ_m (deg)	f_m (Hz)	$T_m = 1/f_m$ (min)
1	200	10	0.00009259	180
2	90	20	0.00020833	80
3	30	30	0.00047619	35
4	17	40	0.00111111	15
5	8	50	0.00238095	7
6	3.5	60	0.00555555	3
7	1	70	0.025	2/3

that we can use to generate an exact analytic solution for the geoelectric field that will be produced. From Fourier's theorem we know that any function can be represented as a sum of cosine and sine functions [28]. Studies of geomagnetic disturbances have shown spectra with the amplitude decreasing with increasing frequency [26]. To provide a synthetic magnetic field variation that reproduces this behaviour, we define a test magnetic field variation as the sum of seven sine waves:

$$B(t) = \sum_{m=1}^{7} A_m \sin(2\pi f_m t + \Phi_m) \tag{20}$$

with amplitudes, A_m, approximately proportional to $1/f_m$, and phases, Φ_m, assigned arbitrary values as shown in Table 1. The amplitudes and phases of the frequency components are also shown in Fig. 1. The rate of change of the magnetic field, $dB(t)/dt$, is easily obtained from (20) and is given by

$$\frac{dB(t)}{dt} = \sum_{m=1}^{7} 2\pi f_m A_m cos(2\pi f_m t + \Phi_m) \tag{21}$$

IV. EARTH RESPONSE

As shown in Section II, the Earth transfer function K(f), as well as the magnetotelluric relation C(f), can be determined exactly in the case of a multi-layer Earth using a recursive relation, and if the Earth is uniform K(f) and C(f) even have simple explicit formulas. To provide Earth responses for testing geoelectric field calculations, we use two Earth models: (1) with a uniform conductivity, and (2) with layers of different conductivities.

A. MODEL 1: UNIFORM EARTH, RESISTIVITY = 1000 ω-m

As a first approximation to the Earth conductivity, in the absence of more specific information, the Earth can be modelled as a uniform half-space with a specified resistivity. The resistivities within the crust of the Earth can range from 100 to 10,000 Ωm, so an average value of 1000 Ωm is often used. The transfer function is then simply obtained from (13), and equation (8) gives the magnetotelluric relation.

B. MODEL 2: LAYERED EARTH, QUÉBEC MODEL

To provide a higher resolution Earth model for geomagnetic hazard assessments, it is possible to use a layered-Earth

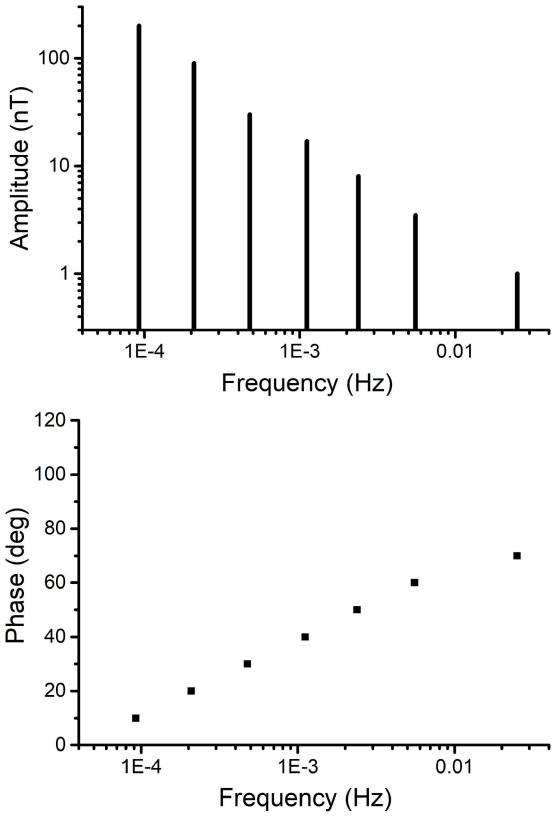

FIGURE 1. Spectrum for synthetic test magnetic field variation: a) Amplitude, b) Phase.

model that represents the variation of Earth conductivity with depth. An example of such a model is the one for Québec that has been used in a number of studies e.g. [29], [30]. This model consists of 5 layers with, from the top down, thicknesses and resistivities: 15 km, 20,000 Ωm; 10 km, 200 Ωm; 125 km, 1000 Ωm; 200 km, 100 Ωm; above a half space of 3 Ωm. The transfer function in this case is given by the recursive relation (19), and equation (8) can again be used for determining the magnetotelluric relation.

C. EARTH RESPONSE FUNCTIONS

The transfer functions for Models 1 and 2 are shown in Fig. 2 for the range of frequencies relevant to GIC. Similarly, Fig. 3 shows the magnetotelluric relation for the two models. For the frequencies in the test magnetic field spectrum, the transfer function $K(f)$ values for a uniform Earth, from (13), are shown in Table 2, while the values of $K(f)$ for a multi-layer Earth, from the recursive relation (19), are shown in Table 3. The values for the magnetotelluric relation $C(f)$, for a uniform Earth, from (8), are shown in Table 4, while the values of $C(f)$ for a multi-layer Earth, from (8), are shown in Table 5.

V. GEOELECTRIC FIELD

The geoelectric field depends on the geomagnetic field variation and the transfer function of the Earth as shown in equation (6). Thus each frequency component of the test

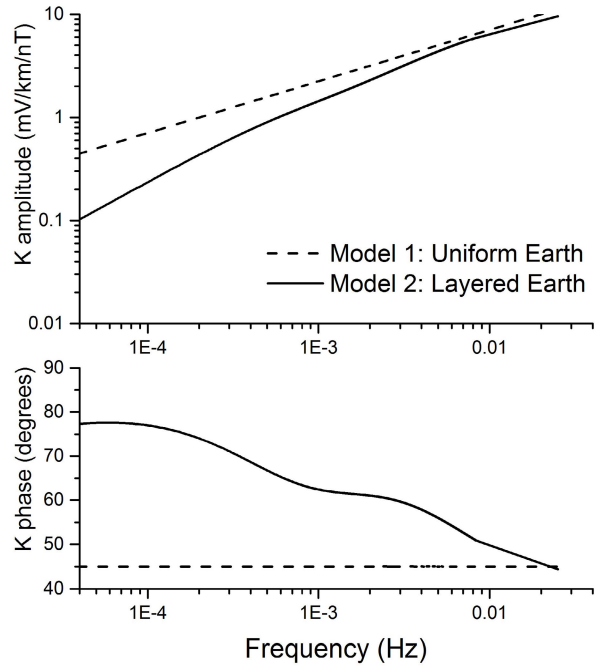

FIGURE 2. Amplitude and phase of the transfer function $K(f)$ for a 1000 Ωm uniform Earth (dashed lines) and for a multi-layer Earth (5-layer Québec model) (solid lines).

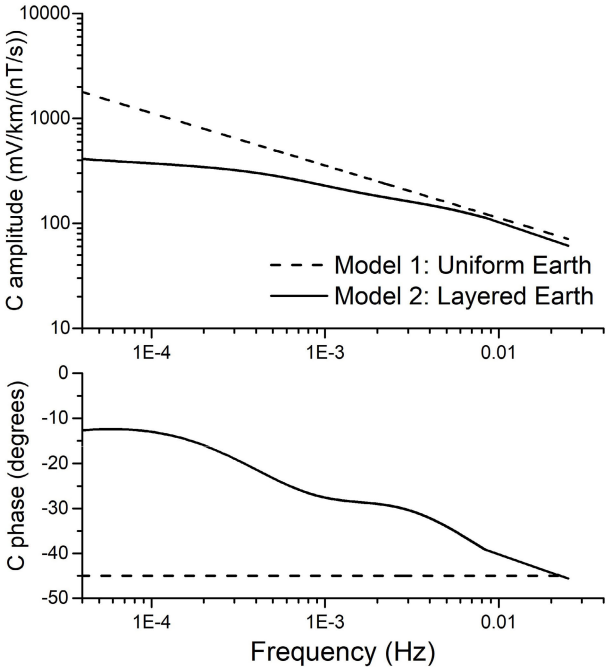

FIGURE 3. Amplitude and phase of the magnetotelluric relation $C(f)$ for a 1000 Ωm uniform Earth (dashed lines) and for a multi-layer Earth (5-layer Québec model) (solid lines).

magnetic field waveform (20), with amplitudes and phases given by Table 1, is combined with the corresponding transfer function value. The resulting geoelectric field is given by

$$E(t) = \sum_{m=1}^{7} |K_m| A_m sin(2\pi f_m t + \Phi_m + \theta_m) \qquad (22)$$

TABLE 2. Transfer function $K(f)$ for the frequencies in the synthetic test magnetic field variation for a 1000 Ωm uniform Earth.

m	f_m (Hz)	Amplitude $\|K_m\|$ (mV/km/nT)	Phase, θ_m (deg)
1	0.000093	0.6804	45.00
2	0.000208	1.0206	45.00
3	0.000476	1.5430	45.00
4	0.001111	2.3570	45.00
5	0.002381	3.4503	45.00
6	0.005556	5.2705	45.00
7	0.025	11.1803	45.00

TABLE 3. Transfer function $K(f)$ for the frequencies in the synthetic test magnetic field variation for a multi-layer Earth (5-layer Québec model).

m	f_m (Hz)	Amplitude, $\|K_m\|$ (mV/km/nT)	Phase, θ_m (deg)
1	0.000093	0.2188	77.15
2	0.000208	0.4480	73.76
3	0.000476	0.8681	67.17
4	0.001111	1.5392	62.08
5	0.002381	2.5935	60.58
6	0.005556	4.6625	54.97
7	0.025	9.6047	44.38

TABLE 4. Magnetotelluric relation $C(f)$ for the frequencies in the synthetic test magnetic field variation for a 1000 Ωm uniform Earth.

m	f_m (Hz)	Amplitude, $\|C_m\|$ (mV/km/(nT/s))	Phase, θ_m (deg)
1	0.000093	1169.545	-45.00
2	0.000208	779.697	-45.00
3	0.000476	515.721	-45.00
4	0.001111	337.619	-45.00
5	0.002381	230.637	-45.00
6	0.005556	150.988	-45.00
7	0.025	71.176	-45.00

TABLE 5. Magnetotelluric relation $C(f)$ for the frequencies in the synthetic test magnetic field variation for a multi-layer Earth (5-layer Québec model).

m	f_m (Hz)	Amplitude, $\|C_m\|$ (mV/km/(nT/s))	Phase, θ_m (deg)
1	0.000093	376.153	-12.85
2	0.000208	342.275	-16.24
3	0.000476	290.126	-22.83
4	0.001111	220.474	-27.92
5	0.002381	173.364	-29.42
6	0.005556	133.570	-35.03
7	0.025	61.145	-45.62

where the transfer function amplitude, $|K_m|$ and phase θ_m are given by Table 2 for a uniform Earth and by Table 3 for a multi-layer Earth. Multiplying the $|K_m|$ and

TABLE 6. Parameters of electric field waveform for a 1000 Ωm uniform Earth.

m	f_m (Hz)	Amplitude, E_m (mV/km)	Phase,φ_m (deg)
1	0.000093	136.08276	55.00
2	0.000208	91.85587	65.00
3	0.000476	46.29100	75.00
4	0.001111	40.06938	85.00
5	0.002381	27.60262	95.00
6	0.005556	18.44662	105.00
7	0.025	11.18034	115.00

TABLE 7. Parameters of electric field waveform for a multi-layer Earth (5-layer Québec model).

m	f_m (Hz)	Amplitude, E_m (mV/km)	Phase, φ_m (deg)
1	0.000093	43.76735	87.15
2	0.000208	40.32326	93.76
3	0.000476	26.04161	97.17
4	0.001111	26.16634	102.08
5	0.002381	20.74819	110.58
6	0.005556	16.31864	114.97
7	0.025	9.60469	114.38

A_m terms and adding the phases in (22) gives the geoelectric field

$$E(t) = \sum_{m=1}^{7} E_m sin(2\pi f_m t + \varphi_m) \quad (23)$$

with the amplitudes E_m and phases φ_m as given in Table 6, for a uniform Earth, and in Table 7 for a multi-layer Earth. The amplitudes and phases of the frequency components are also shown in Figs. 4 and 5.

VI. TESTING GEOELECTRIC FIELD SOFTWARE

The formulas derived in the previous sections are designed to be applied for testing software used in calculating geoelectric fields from geomagnetic field measurements and a 1-D model of Earth conductivity. Equation (20) can be used to generate a set of synthetic test magnetic field data to use as input to the software. The software can then be applied with the uniform or multi-layer Earth to calculate the geoelectric field that would be produced by these magnetic field data. Equation (23) with the parameters from Table 6 or Table 7 can then be used to calculate the exact geoelectric field values that would be produced, and these can be compared with the output of the software.

The standard output from magnetic observatories is magnetic field values measured with a sampling interval of 1 minute. Magnetic field measurements are also made with sampling intervals of 1 second, 5 seconds and 10 seconds. Equation (20) enables generating magnetic field data with any of these sampling intervals. The duration of the data set can be chosen to match typical data lengths for which the software is designed to operate.

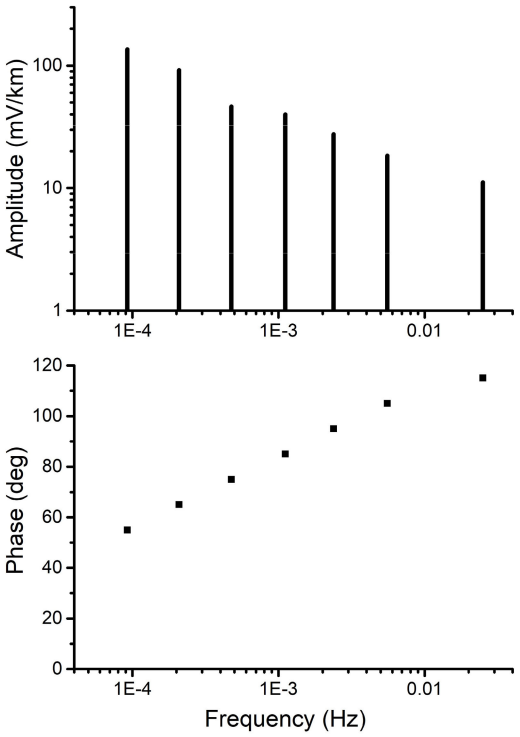

FIGURE 4. Spectrum for test electric field variations in the case of a 1000 Ωm uniform Earth a) Amplitude, b) Phase.

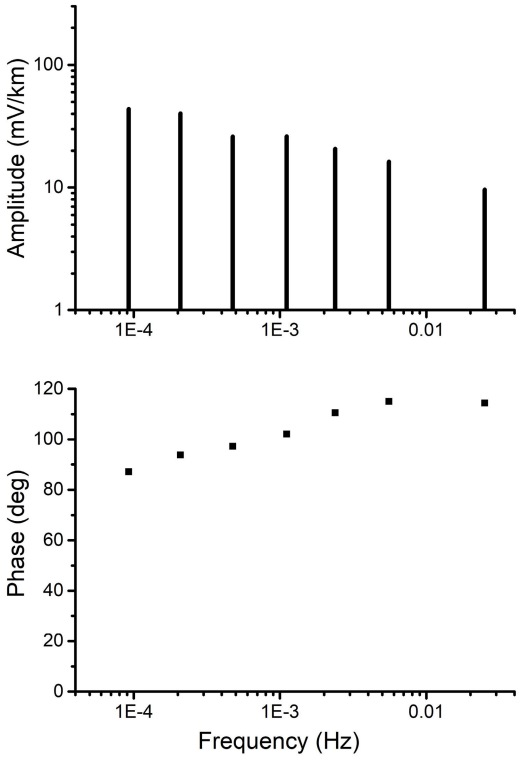

FIGURE 5. Spectrum for test electric field variations for a multi-layer Earth (5-layer Québec model) Amplitude, b) Phase.

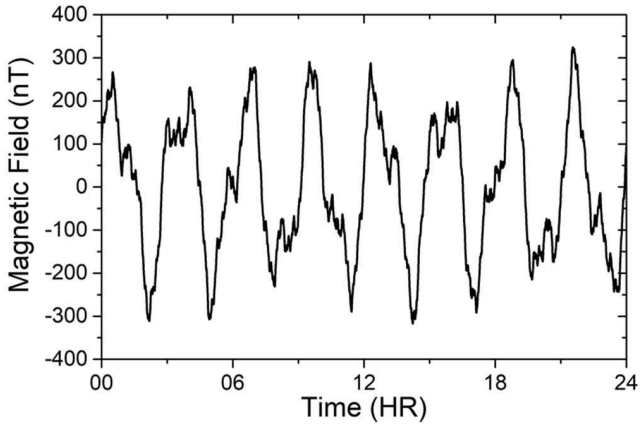

FIGURE 6. Synthetic test geomagnetic field variation obtained from equation (20) with the parameter values in Table 1. The centre day of the 3-day dataset is shown.

As an example of using the test data, consider testing software designed to work with magnetic data with a sampling interval of 1 second and to calculate geoelectric field values for a complete Universal Time (U.T.) day. Equation (20) is used to generate magnetic field data for 3 consecutive days. Fig 6 shows the magnetic field variations on the centre day. The magnetic field data can be used with the uniform or layered Earth model to calculate the geoelectric fields. The exact geoelectric fields for these two cases, given by (23) with the parameters from Table 6 or Table 7, are shown in Figures 7a and 7b.

The data sets obtained are provided on the IEEE DataPort. It is necessary to emphasize, referring to Section II.B, that B expressed by equation (20) with the parameter values given in Table 1 and shown in Fig. 6 and E expressed by equation (23) with the parameter values given in Table 6 or Table 7 and shown in Fig. 7a or Fig. 7b represent either E and B pair: E_x and B_y or $-E_y$ and B_x.

VII. DISCUSSION

Software implementations of geoelectric field calculations often use the 'frequency domain' method because of the computational efficiencies of the Fast Fourier Transform (FFT). An FFT of the geomagnetic field variation gives the magnetic field spectrum, and each spectral component is then multiplied by the corresponding complex value of the Earth transfer function to give the geoelectric field spectrum. An inverse FFT of the geoelectric field spectrum then gives the geoelectric field in the time domain [28].

The geoelectric field can also be calculated directly in the time domain by convolving the geomagnetic field variation with the impulse response of the Earth. The impulse response is the inverse Fourier transform of the Earth response function determined in the frequency domain. We may consider the "High Pass" impulse response associated with the transfer function $K(f)$ or the "Low Pass" impulse response associated with the magnetotelluric relation $C(f)$. The "Low Pass" impulse response, which thus relates the geoelectric field

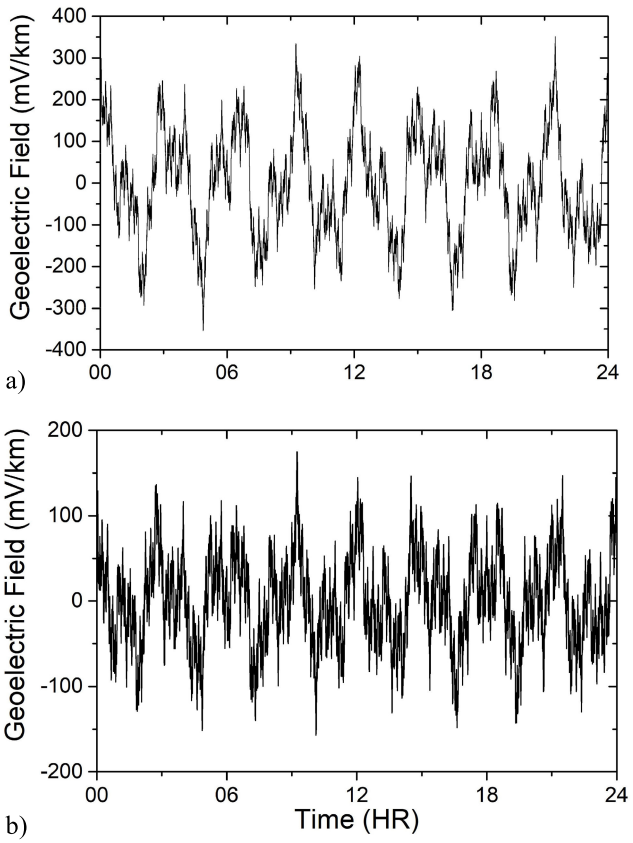

FIGURE 7. Exact geoelectric field obtained from equation (23) with (a) the parameter values given by Table 6 for a 1000 Ωm uniform Earth, and (b) given by Table 7 for a multi-layer Earth (5-layer Québec model). The centre day of the 3-day dataset is shown.

to the rate of change of the magnetic field, dB/dt, can be calculated more easily. The impulse responses can be calculated for a uniform Earth [31] and for a layered Earth [32]. The use of the analytic test calculations shown in this paper has proved valuable in evaluating how the accuracy of the geoelectric field calculation is affected by truncation of the impulse response [31]. It is shown in [31] that, in order to obtain a sufficient accuracy, the "High Pass" impulse response may be truncated much earlier than the "Low Pass" impulse response.

Here we have used a uniform conductivity model and a layered conductivity model to derive analytic solutions that are used to generate the test data. However, the use of the test datasets is not confined to calculations for a uniform or layered Earth. Three-dimensional (3-D) conductivity structures can give rise to geoelectric field and geomagnetic field variations that are not orthogonal. In these cases the geoelectric field and geomagnetic field components are related by a tensor transfer function:

$$\begin{bmatrix} E_x \\ E_y \end{bmatrix} = \begin{bmatrix} K_{xx} & K_{xy} \\ K_{yx} & K_{yy} \end{bmatrix} \begin{bmatrix} B_x \\ B_y \end{bmatrix} \tag{24}$$

Thus the northward component of the geoelectric field, E_x, can be written

$$E_x(f) = E_{xx}(f) + E_{xy}(f) \tag{25}$$

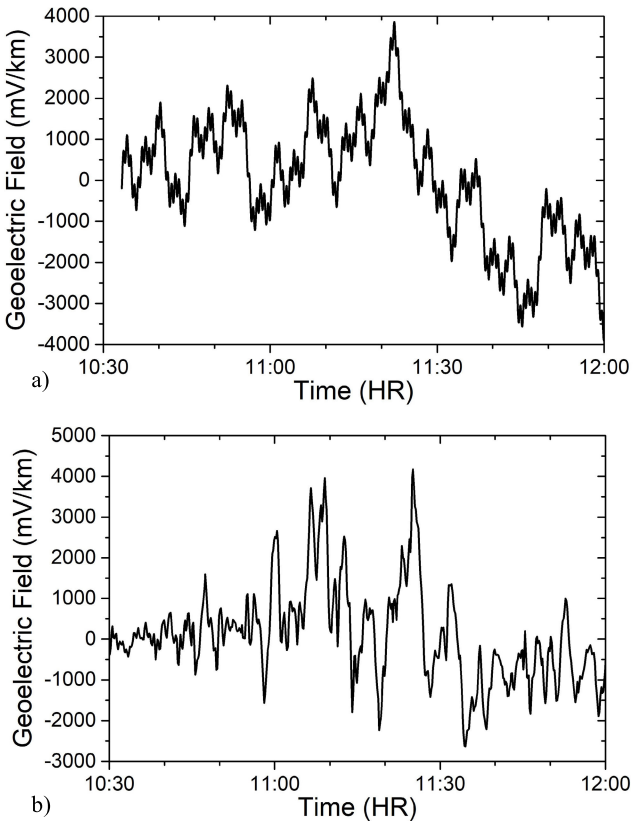

FIGURE 8. Comparison of (a) synthetic electric field and (b) electric field for March 1989, both calculated using the Québec Earth model.

where

$$E_{xx}(f) = K_{xx}(f) B_x(f) \tag{26}$$

$$E_{xy}(f) = K_{xy}(f) B_y(f) \tag{27}$$

Similarly, the eastward component of the geoelectric field, E_y, can be written

$$E_y(f) = E_{yx}(f) + E_{yy}(f) \tag{28}$$

where

$$E_{yx}(f) = K_{yx}(f) B_x(f) \tag{29}$$

$$E_{yy}(f) = K_{yy}(f) B_y(f) \tag{30}$$

It can be seen that these equations are of the same form as equation (6) so the synthetic magnetic field and calculated geoelectric field can be used to test the calculation of the geoelectric field parts given by (26), (27), (29) and (30).

The synthetic geomagnetic field variations and the analytically derived geoelectric fields are both completely artificial. However, the spectrum for the synthetic geomagnetic field variations was chosen to correspond to a typical geomagnetic spectrum found to occur during actual geomagnetic disturbances; thus the synthetic geomagnetic field variations and analytically derived geoelectric fields can be considered representative of the fields occurring during a real geomagnetic disturbance. To illustrate this we calculate the geoelectric field and scale up the values by a factor of 30 to represent a larger event (Fig 8a). This can be compared with the geoelectric field calculated for an interval of the March 13, 1989 geomagnetic storm and shown in Figure 8b. The similarity in the shape of the variations shows that the synthetic geomagnetic field variations presented in this paper could, in principle, be used in other studies as a credible proxy for a real geomagnetic disturbance.

VIII. CONCLUSION

A synthetic geomagnetic field variation has been defined comprising seven frequency components of different amplitudes and phases.

Earth transfer functions for a uniform Earth model and a layered Earth model have been calculated exactly for these seven frequencies.

Combining the formulas for the synthetic geomagnetic field variation and the transfer functions allows the associated geoelectric field to be exactly specified.

The synthetic geomagnetic field variations and the associated geoelectric field can be used as benchmark data sets for testing geoelectric field calculation software [27].

This provides a way of validating software for use in assessing the geomagnetic hazard to power systems and pipelines.

REFERENCES

[1] R. Pirjola, "Geomagnetically induced currents as ground effects of space weather," in *Space Science*, vol. 2, H. J. M. Cuesta, Ed. Rijeka, Croatia: InTech, 2012, pp. 27–44. [Online]. Available: http://www.intechopen.com/books/space-science/geomagnetically-induced-currents-as-ground-effects-of-space-weather

[2] D. H. Boteler, R. J. Pirjola, and H. Nevanlinna, "The effects of geomagnetic disturbances on electrical systems at the Earth's surface," *Adv. Space Res.*, vol. 22, no. 1, pp. 17–27, 1998.

[3] C. W. Anderson, L. J. Lanzerotti, and C. G. Maclennan, "Outage of the L4 system and the geomagnetic disturbances of 4 August 1972," *Bell Syst. Tech. J.*, vol. 53, no. 9, pp. 1817–1837, Nov. 1974.

[4] D. H. Boteler and L. Trichtchenko, "Telluric influence on pipelines," in *Oil and Gas Pipelines: Integrity and Safety Handbook*, R. W. Revie, Ed. Hoboken, NJ, USA: Wiley, 2015, ch. 21, pp. 275–288.

[5] T. S. Molinski, "Why utilities respect geomagnetically induced currents," *J. Atmos. Solar-Terrestrial Phys.*, vol. 64, no. 16, pp. 1765–1778, Nov. 2002.

[6] J. G. Kappenman, "Geomagnetic disturbances and impacts upon power system operation," in *The Electric Power Engineering Handbook*, L. L. Grigsby, Ed., 2nd ed. Boca Raton, FL, USA: CRC Press, 2007, ch. 16-1–16-22.

[7] J. G. Kappenman, "Effects of geomagnetic disturbances on power systems [panel session—PES summer meeting, July 12, 1989 Long Beach, California]," *IEEE Power Eng. Rev.*, vol. 9, no. 10, pp. 15–20, 1989.

[8] B. Bozoki, S. R. Chano, L. L. Dvorak, W. E. Feero, G. Fenner, E. A. Guro, C. F. Henville, J. W. Ingleson, S. Mazumdar, P. G. McLaren, K. K. Mustaphi, F. M. Phillips, R. V. Rebbapragada, and G. D. Rockefeller, "The effects of GIC on protective relaying," *IEEE Trans. Power Del.*, vol. 11, no. 2, pp. 725–739, Apr. 1996.

[9] S. Guillon, P. Toner, L. Gibson, and D. Boteler, "A colorful blackout: The havoc caused by auroral electrojet generated magnetic field variations in 1989," *IEEE Power Energy Mag.*, vol. 14, no. 6, pp. 59–71, Nov./Dec. 2016.

[10] A. Viljanen and R. Pirjola, "Geomagnetically induced currents in the Finnish high-voltage power system," *Surv. Geophys.*, vol. 15, no. 4, pp. 383–408, 1994.

[11] *Effects of Geomagnetic Disturbances on the Bulk Power System*, GMDTF Interim Report, North American Electric Reliability Corporation, Atlanta, GA, USA, 2012.
[12] B. C. Rix and D. Boteler, *Telluric Current Considerations in the CP Design for the Maritimes and Northeast Pipeline*, document NACE-01317, Houston, TX, USA, Mar. 2001.
[13] R. Horton, D. Boteler, T. J. Overbye, R. Pirjola, and R. C. Dugan, "A test case for the calculation of geomagnetically induced currents," *IEEE Trans. Power Del.*, vol. 27, no. 4, pp. 2368–2373, Oct. 2012.
[14] D. H. Boteler, "A new versatile method for modelling geomagnetic induction in pipelines," *Geophys. J. Int.*, vol. 191, no. 2, pp. 98–109, Nov. 2012. doi: 10.1093/gji/ggs113.
[15] L. Cagniard, "Basic theory of the magneto-telluric method of geophysical prospecting," *Geophysics*, vol. 18, no. 3, pp. 605–635, 1953.
[16] J. R. Wait, "On the relation between telluric currents and the Earth's magnetic field," *Geophysics*, vol. 19, no. 2, pp. 281–289, 1954.
[17] A. T. Price, "The theory of magnetotelluric methods when the source field is considered," *J. Geophys. Res.*, vol. 67, no. 5, pp. 1907–1918, 1962.
[18] J. R. Wait, "Theory of magneto-telluric fields," *J. Res. Nat. Bur. Standards—D. Radio Propag.*, vol. 66D, no. 5, pp. 509–541, Sep./Oct. 1962.
[19] A. A. Kaufman and G. V. Keller, "The magnetotelluric sounding method," in *Methods in Geochemistry and Geophysics*, vol. 15. Amsterdam, The Netherlands: Elsevier, 1981.
[20] F. Simpson and K. Bahr, *Practical Magnetotellurics*, 1st ed. Cambridge, U.K.: Cambridge Univ. Press, 2005, p. 272.
[21] V. D. Albertson and J. A. Van Baelen, "Electric and magnetic fields at the Earth's surface due to auroral currents," *IEEE Trans. Power App. Syst.*, vol. PAS-89, vol. 4, pp. 578–584, Apr. 1970.
[22] K. Zheng, R. J. Pirjola, D. H. Boteler, and L. G. Liu, "Geoelectric fields due to small-scale and large-scale source currents," *IEEE Trans. Power Del.*, vol. 28, no. 1, pp. 442–449, Jan. 2013. doi: 10.1109/TPWRD.2012.2226248.
[23] R.-U. Börner, "Numerical modelling in geo-electromagnetics: Advances and challenges," *Surv. Geophys.*, vol. 31, no. 2, pp. 225–245, 2010.
[24] J. T. Weaver, *Mathematical Methods for Geo–Electromagnetic Induction*. Taunton, U.K.: Research Studies Press, 1994.
[25] L. Trichtchenko and D. H. Boteler, "Modelling of geomagnetic induction in pipelines," *Annales Geophysicae*, vol. 20, no. 7, pp. 1063–1072, 2002.
[26] D. H. Boteler, "Geomagnetically induced currents: Present knowledge and future research," *IEEE Trans. Power Del.*, vol. 9, no. 1, pp. 50–58, Jan. 1994.
[27] D. H. Boteler and R. J. Pirjola, "Numerical calculation of geoelectric fields that affect critical infrastructure," *Int. J. Geosci.*, vol. 10, no. 10, Oct. 2019.
[28] R. Bracewell, *The Fourier Transform & Its Applications*, 2nd ed. New York, NY, USA: McGraw-Hill, 1978, p. 444.
[29] D. H. Boteler, "Assessment of geomagnetic hazard to power systems in Canada," *Natural Hazards*, vol. 23, nos. 2–3, pp. 101–120, 2001.
[30] A. Pulkkinen, E. Bernabeu, J. Eichner, C. Beggan, and A. W. P. Thomson, "Generation of 100-year geomagnetically induced current scenarios," *Space Weather*, vol. 10, no. 4, pp. 1–19, Apr. 2012.
[31] R. J. Pirjola and D. H. Boteler, "Truncation of the earth impulse responses relating geoelectric fields and geomagnetic field variations," *Geosci. Res.*, vol. 2, no. 2, pp. 72–92, 2017.
[32] L. Marti, A. Rezaei-Zare, and D. Boteler, "Calculation of induced electric field during a geomagnetic storm using recursive convolution," *IEEE Trans. Power Del.*, vol. 29, no. 2, pp. 802–807, Apr. 2014.

DAVID H. BOTELER was born in London, U.K. He received the B.Sc. degree in electronic engineering from the University of Wales, the M.Sc. degree in geophysics from The University of British Columbia, Canada, and the Ph.D. degree in physics from the Victoria University of Wellington, New Zealand. Since 1990, he has been a Research Scientist with Natural Resources Canada specializing in space weather and geomagnetic effects on technological systems. He is an Associate of the Infrastructure Resilience Research Group, Carleton University, Ottawa. He has over 30 years' experience working on interdisciplinary problems, including work in the Antarctic and Arctic. He was the Director of the International Space Environment Service (ISES), from 2002 to 2012.

RISTO J. PIRJOLA was born in Helsinki, Finland, in 1950. He received the M.Sc. degree in mathematics and the Ph.D. degree in theoretical physics from the University of Helsinki, Finland, in 1971 and 1982, respectively. From 1978 to 2016, he was a Scientist and Research Manager with the Finnish Meteorological Institute, Helsinki, including long-term scientific visits to Natural Resources Canada, Ottawa, where he has been a Physical Science Expert, since 2017. He is an author or a coauthor of about 125 peer-reviewed articles and about 135 other publications. His research interests include geoelectromagnetic fields and geomagnetically induced currents.

LUIS MARTI (F'15) received the M.A.Sc. and Ph.D. degrees in electrical engineering from The University of British Columbia, in 1983 and 1987, respectively. He was with Ontario Hydro (now Hydro One) from 1989 to 2016, where he was responsible for the Special Studies Group. His research interests include development of models for the family of EMTP programs, GIC simulation, grounding, induction coordination, EMF issues pertaining to T & D networks, and technical issues around the connection of renewable generation in distribution networks. He has participated in a number of Canadian and international technical organizations, such as Canadian Standards Association, IEEE, and CIGRE. He has served as the Vice Chair of the NERC GMD standard development team for TPL-002 and an Adjunct Professor at the Universities of Toronto, Waterloo, Western Ontario, and Ryerson. He is currently the President of a consulting firm focusing on GMD-and EMTP studies/research.